U.M. Nayef
Department of Applied Science, University of Technology, Baghdad, Iraq.

A.M. Abdul Hussein
Department of Applied Science, University of Technology, Baghdad, Iraq.

A.J. Kata
Department of Applied Science, University of Technology, Baghdad, Iraq.
unayef@yahoo.com

Received on: 05/01/2016
Accepted on: 19/05/2016

Preparation and Characterization Study of Porous Silicon Doped with Cu and Ag

Abstract*-In this paper, porous silicon was prepared by using electrochemical etching technique of p-type silicon acceptor, with a resistivity of 1.5-4Ohm.cm, using hydrochloric acid with concentration of 24%. The etching current density effect 4, 12, 20mA/cm2 was carried out at constant etching time of 15min. The structural characteristics of the porous silicon and the doped porous silicon were studied and found an expansion in the spectrum of the X-rays and a simple shift in the diffraction angles while maintaining the surface direction (111). The morphological properties were studied using the atomic force microscope which showed pores formation and gives the pore diameter within the range of 19.08 to 44.73nm for the prepared samples. It was also noted that the rate of pore diameter and the thickness of the porous silicon layer increased with increasing etching current density. Electrical characteristics of the nanoscale porous silicon layer and the doped porous silicon with silver and copper showed that Current-Voltage (I-V) characteristics of the prepared samples to be a rectifying behavior. An improvement in the electrical characteristics of the doped porous silicon samples was observed*

Keywords*- Porous silicon; Doping; Morphological; Electrical properties.*

How to cite this article: U.M. Nayef, A.M. Abdul Hussein and A.J. Kata, "Preparation and Characterization Study of Porous Silicon Doped with Cu and Ag," *Engineering and Technology Journal*, Vol. 35, Part B, No. 1, pp. 8-12, 2017.

1. Introduction

Silicon (Si) as nanomaterial stills an important structure especially for semiconductor industry. It is well recognized as auspicious building blocks for equipment in the fields of energy conversion [4], nanoelectronics [1,2] opto-electronics [3], and energy storage,[5], besides bio and chemical sensors [6]. A number of characteristic parameters effect the properties of the Si nanostructure. These parameters are crystalline orientation [7] crystalline quality [8] strain [9] orientation relative to the substrate [10] and size affect [11]. Thus, they are important for their application in many devices. Porous silicon is broken down into three classifications as outlined by (IUPAC). The classification is determined by the pore diameter (d) which can be defined as the distance between two opposing walls also referred to as inside diameter (ID). Class one is microporous (d < 2nm), class two mesoporous (2nm<d< 50nm) and class three is macroporous (d > 50nm) [12].

The creation of multifunctional nano-composite with metals doped porous silicon is vital process. These transition-metal ions such as Cu or Ag, which are presented in porous silicon (PS) layer, may offer new nanostructure with optical, electrical and magnetic properties. Familiar doping methods (Immersion or Electro-deposition) are presently applied. These must be followed by a heat treatment to endorse the insertion of the metal ions inside the porous matrix and to form metal oxides at the porous surface [13]. In this research, porous silicon is preparing by electrochemical etching technique of p-type silicon acceptor, using hydrochloric acid
with different etching current density at constant time.

2. Experimental Part

The PS samples used in these experiments were formed on the polished surfaces of (111) oriented p-type wafers of 500±50μm thickness with resistivity ρ=1.5-4 Ω.cm. Before etching process, the silicon wafers were rinsed with ethanol and action to remove dirt followed by dilute 24% hydrofluoric (HF) acid to eliminate the native oxide layer and dried by nitrogen. Aluminum film was deposited on the backside of silicon wafers in order to creating an ohmic contact. This has been achieved by using thermal evaporation process in vacuum chamber (10-5torr). The silicon wafer has been cut out into small pieces in different dimensions. After finishing the etching process, the samples have been rinsed with ethanol and pentane and dried using nitrogen gas.PS samples have been produced by the electrochemical etching process. Figure 1 represents the experiment setup for the electrochemical etching. Silver nitrate ($AgNO_3$) (High purity 99.99%) of 169.87g/mol and copper nitrate $Cu(NO_3)_2$ (High purity 99.99%) of (187.55g/mol) molecular weight, was dissolved in D.D water and used to synthesis solution with different (10-2, 10-3 and 1.5×10-3 M) 20 ml add to 24% HF acid for the PS doped preparing.

https://doi.org/10.30684/etj.35.1B.2
2412-0758/University of Technology-Iraq, Baghdad, Iraq
This is an open access article under the CC BY 4.0 license http://creativecommons.org/licenses/by/4.0

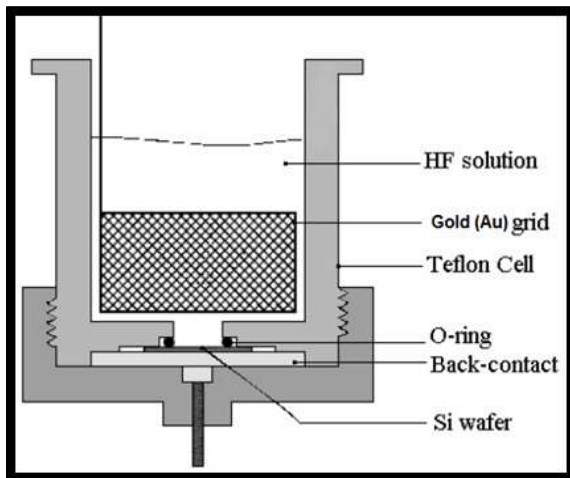

Figure 1: Schematic diagram of Porous silicon Anodization Cell

Form XRD peak, we can know the lattice constant and miller indices from the eq.

$2d\sin\theta = n'\lambda$ (1) (Bragg's law)

$a = d(\sqrt{h^2+k^2+l^2})$ (2) (Lattice constant for cubic structure)

Where λ: the wavelength of X-ray was beam (0.154606 nm), θ: is the scattering angle, n': is order of diffraction peak, d: is interplane distance (nm), a: lattice constant (nm) from Scherrer-debay eq. (3). We can find the crystallites size of PS by measuring the full width at half maximum (FWHM) of the peak

$G.S = k\lambda / B\cos\theta$ (3) (Scherrer eq.)

Where G.S: crystallites size (nm) and B: is FWHM and k: is a constant (k=0.89).

3. Results and Discussion

I. Structural Properties

From the Figure (2a,b) these are a distinct variation between the bulk silicon surface and the PS surfaces formed at 12mA/cm2 anodizing current density for 15min with 24% HF concentration. XRD spectra of bulk silicon shows a very sharp peak at 2θ=28.537o while the porous silicon shows the peak at 2θ=28.695o (according to JCPDS: 27-1402) [14], which viewing the single crystalline nature of the silicon at preferred orientation (111). The crystallite size presents the remnant silicon portion after the dissolution and formation of pores. Furthermore, the presences of this peak in all the PS structures approved that the cubic structure of the crystalline silicon is retained even after the pore formation [15]. The porous structure and the decrease of the Si size caused a broadening of the Si plane (111) peak, and slightly shifted to higher diffraction angle than the bulk Si peak. The adding of HF acid into the solution for copper doping PS permits the removal of SiO_2. It also permitted the continuous deposition of copper besides silicon dissolution. This process is usually named as displacement deposition due to the nonstop substitution of the substrate's atoms with the metal's ions [16]. Previous researches have also shown the copper was deposited by displacement on the surface of PS in the form of crystalline NPs [17]. The pore channels bounded the size of NPs. In fact, the final material of copper or silver displacement deposition on PS represented the layer of the Cu/PS or Ag/Cu nanocomposites. The initial stages of deposition were accompanied by the formation of metal particles of some nanometers diameter inheriting the crystallographic orientation of the PS skeleton [18]. Additional copper particles growth leads to the (111) prevalence orientation of the copper deposit [19], therefore the grain size of PS doped with copper will be reduce as appear in Figure 2c. The standard and experimental interplaner distances (d) and lattice constant (a) of bulk Si, PS and doped Ps listed in Table1, while Table 2 shows the full width at half maximum (FWHM) and crystallites size of bulk Si, PS and doped Ps layers.

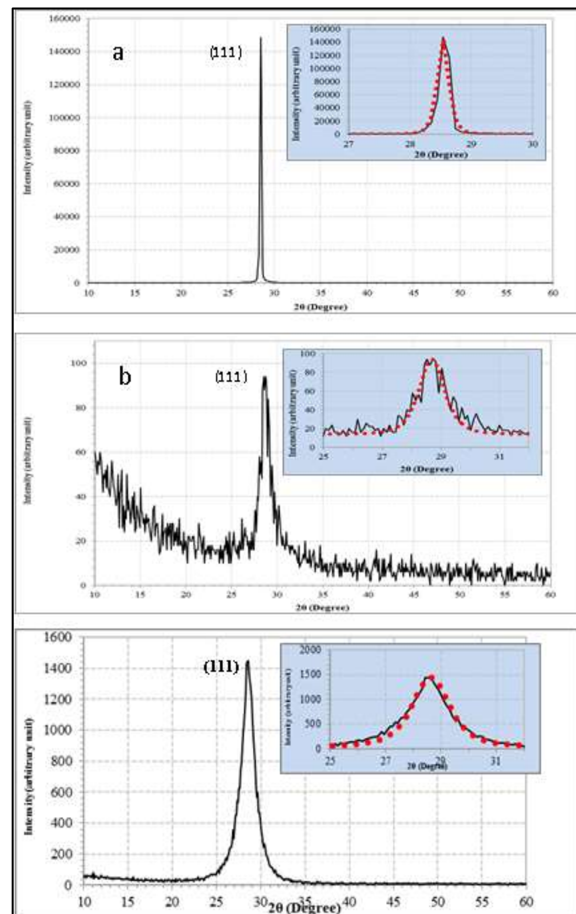

Figure 2: XRD pattern of (a) c-Si (bulk), (b) PS, (c) PS doped with Cu

Table 1: The interplaner distance (*d*) and lattice constant (*a*) of bulk Si, PS and doped PS.

Samples	2θ (deg.)	d_{hkl} Exp. (nm)	d_{hkl} Std. (nm)	hkl	phase	*a* nm)
c-Si (Bulk)	28.537	0.31254	0.31474	(111)	Cub. Si	0.54133
PS	28.695	0.31085	0.31474	(111)	Cub. Si	0.53841
PS:Ag	28.635	0.31149	0.31474	(111)	Cub. Si	0.53952
PS:Cu	28.438	0.31360	0.31474	(111)	Cub. Si	0.54318

Table 2: Crystallites size obtained by means of Scherrer equation of bulk Si, PS and doped PS layers.

Samples	2θ (deg.)	FWHM (deg.)	G.S (nm)
c-Si	28.537	0.149	61.1
PS	28.695	0.9655	9.4
PS:Ag	28.635	1.5385	5.9
PS:Cu	28.438	1.7808	5.1

II. Morphological Properties of PS and doped PS

Figure 3 Shows the AFM 3D images topographies for samples of doped PS. It can found that PS is completely covered by plentiful porous structures. A lot of generated Ag^{+} and Cu^{+2} ions spreaded throughout the nanowires of PS. Subsequently, it nucleates on the surface of PS using the Ag and Cu nanoparticles catalysis, and the pore structures maybe formed around the nanowires. In the meantime, the density of Si nanowires is decreased in comparison to that of Figure (3a) this is attributed to extreme dissolution of PS. The lengths of Si nanowires are not very uniform, and found to be longer than that of Fig. (3a) it shows that the reaction driving force is larger in this case.

Topographies exhibit a remarkable difference in the surface morphology after formation of porous silicon proved by pillar nanostructures with different nanometer sizes. It were clearly seen that the pore size expands when the doped samples by Ag^{+} ions and Cu^{+2} ions; the morphology of substrates which have undergone a deposition of Ag and Cu nanoparticles, illustrated in Table 3.

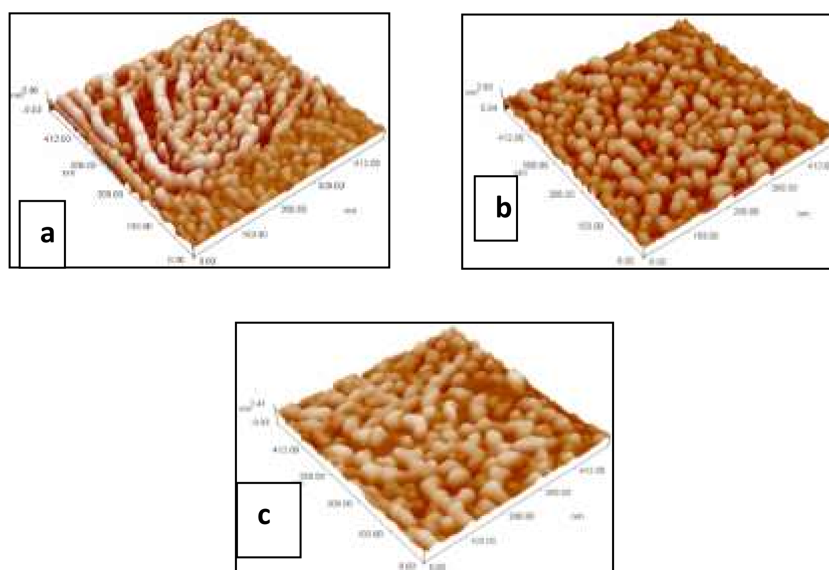

Figure 3: AFM 3D images of (a) PS without doping (b) PS doped with 0.01M of $Cu(NO_3)_2$ (c) PS doped with 0.01M of $AgNO_3$ at current density 12mA/cm^2 and etching time 15min

Table 3: Average diameter and average roughness of all prepared samples

Sample	HF %	Time (min)	Current Density (mA/cm^2)	Average Diameter (nm)	Average Roughness (nm)
PS				23.39	1.24
PS:0.01M$AgNO_3$	24	15	12	34.42	0.355
PS:0.01M$Cu(NO_3)_2$				34.35	0.318

III. Electrical Properties

From Figures (4-6) when increasing the current density of etching, the output current also decreasing and this due to increasing in thickness of PS layer and increasing in resistivity of PS (increasing in interface traps density). In addition, these Figures show a rectifier contact between PS, Al, and this due to the formation of a junction like isotope hetrojunction [20]. The formation of heterojunction structure in this case goes to the quantum confinement in silicon nanocrystallites. This is because the porous layer has a much broader energy gap than that of the *c*-Si. Hence, the PS/*c*-Si maybe considered as a heterojunction between two semiconductors with different forbidden gaps [21].

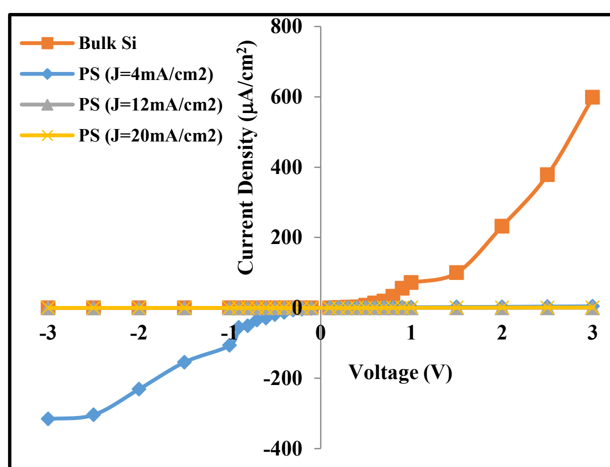

Figure 4: J-V characteristic under dark for bulk Si, and PS samples with current density 4, 12 and 20mA/cm²

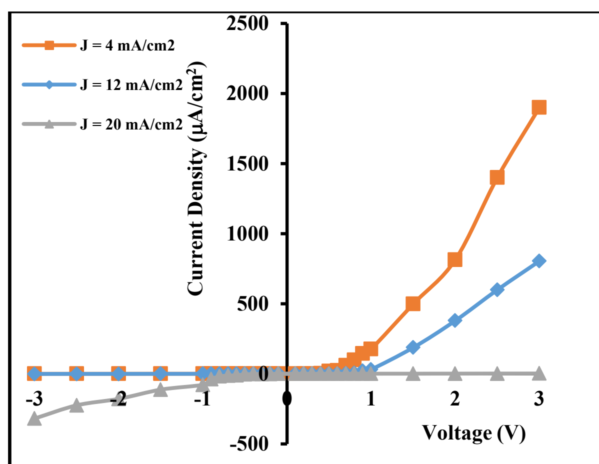

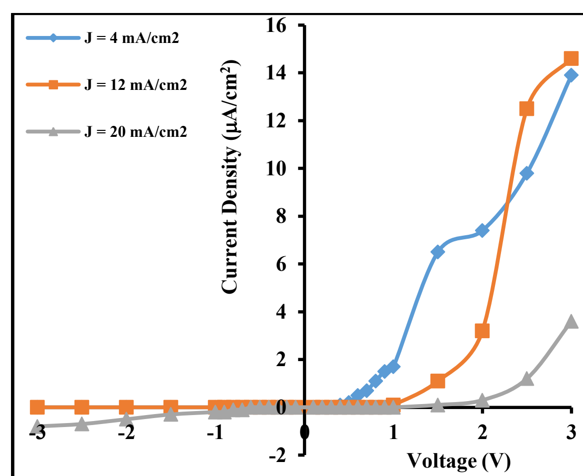

Figure 6: J-V characteristic under dark for PS doped with0.01M of $Cu(NO_3)_2$ with current density of 4, 12 and 20mA/cm²

Figure 7, represent the *J*-V characteristics illumination with different power intensities (5, 20, 60 & 125mW/cm²) at room temperature of Al/doped PS/p-Si/Al sandwich structure, studied with copper and silver doping in PS with different concentrations. The photocurrent curves were obtained by applying a varying reverse bias (0V to -3*V*) and measurement the output current. When the structures were illuminated, the electron-holes pairs are formed in the PS/*c*-Si depletion [22]. In forward bias, this will have no effect since the current is limited by the resistance of PS layer. In the reverse bias, the current is increased, especially at high voltage where the barrier is the main illumination for the current. In addition, it is noticed that increasing the light intensity results increase the photocurrent. This can be ascribed to increasing the generated photo-carriers [23].

Figure 5: J-V characteristic under dark for PS doped with 0.01M of $AgNO_3$ with current density of 4, 12 and 20mA/cm^2

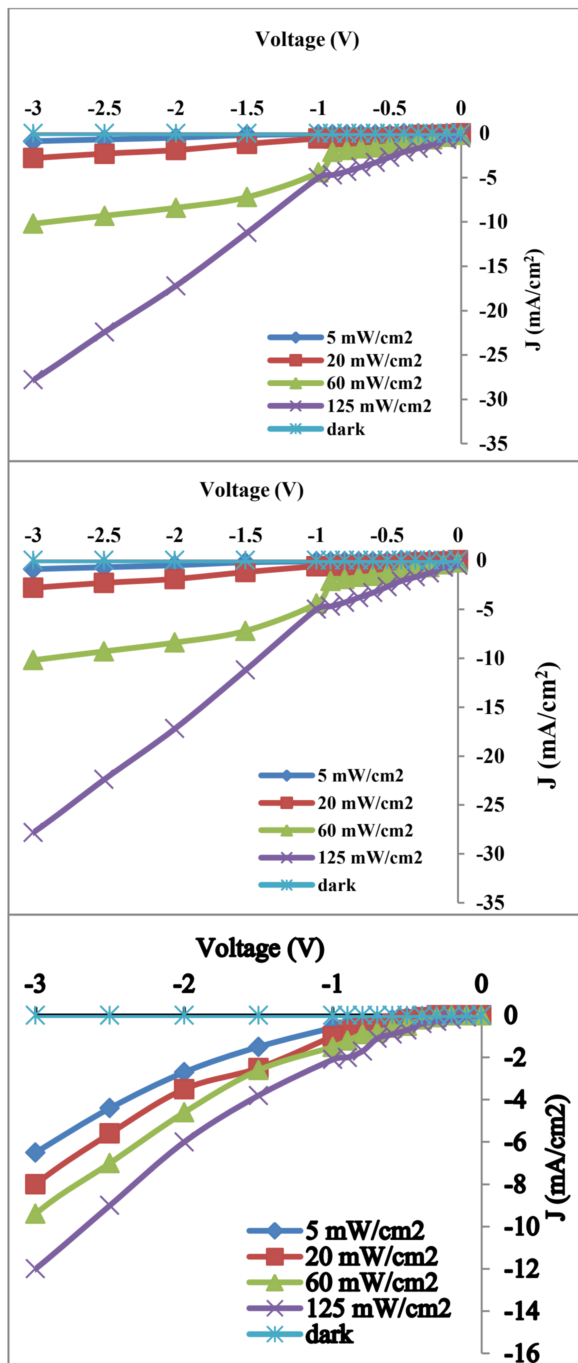

Figure 7: J_{ph}-V characteristic under illumination for of PS, PS doped with0.01M of $AgNO_3$ and PS doped with 0.01M of $Cu(NO_3)_2$ at current density of 12mA/cm^2 and etching time 15min

4.Conclusions

1. XRD spectral show that PS peak become broad due to smaller particles size. This is because the size effect and straining the peaks become broader and widths larger when compared with c-Si due to the shifting of diffraction angle in nano-walls between pores of PS layers.
2. We found that the surface morphology of the PS layer is strongly depends on fabrication conditions.
3. Doping is another parameter that can control or improve the conductivity of the porous silicon PS layer doped with Ag and Cu has the lower electrical resistivity.

References

[1].V. Schmidt, H. Riel, S. Senz, S. Karg, W. Riess, U. Gösele, Small, 2, 85, 2005.
[2].J. Goldberger, A. I. Hochbaum, R. Fan, P. Yang, Nano Lett., 6, 973, 2006.
[3].B. Tian, X. Zheng, T. J. Kempa, Y. Fang, N. Yu, G. Yu, J. Huang, C. M. Lieber, Nature 2007, 449, 885.
[4].K. Q. Peng, Y. Xu, Y. Wu, Y. J. Yan, S. T. Lee , J. Zhu , Small, 1, 1062, 2005.
[5].Y. Cui, Q. Wei, H. Park, C. M. Lieber, Science, 293, 1289, 2001.
[6].C.K. Chan, H.L. Peng, G. Liu, K. McIlwrath, X.F. Zhang, R.A. Huggins, Y. Cui, Nat. Nanotechnol, 3, 31, 2008.
[7].S.G. Cloutier, C.H. Hsu, P.A. Kossyrev, J. Xu, Adv. Mater,18, 841, 2006.
[8].K.H. Hong, J. Kim, S,H. Lee, J.K. Shin, Nano Lett., 8, 1335.
[9].H. Fang, X. D. Li, S. Song, Y. Xu, J. Zhu, Nanotechnology, 19, 255703, 2008.
[10].D.D.D. Ma, C.S. Lee, F.C.K. Au, S.Y. Tong, S.T. Lee, Science, 299, 1874, 2003.
[11].Kevin Luongo, M.Sc. Thesis, University of South Florida, 2006.
[12].M-B Bouzourâa, M. Rahmani, M.-A Zaïbi, N. Lorrain, L. Hajji, M. Oueslati, Journal of Luminescence 143, 521-525, 2013.
[13].M. Jayachandran, M. Paramasivam, K.R. Murali, D.C. Trivedi, and M. Raghavan, Mater Phys. Mech.4, 143-147, 2001.
[14].N.A. AL-Temeeme, S.M. Ghaida, “Study of Some Structural Properties of Porous Silicon Preparing by Photochemical Etching”, Iraqi Journal of Physics, Vol.7, No 8, 44- 52, 2009.
[15].Magagnin L, Maboudian R, CarraroC,Electrochem Solid State Lett, 4(1):C5–C7, 2001.
[16].Bandarenka H, Balucani M, Crescenzi R, Ferrari A, Superlattices Microstruct, 44:583, 2008.
[17].Bandarenka H, Prischepa S, Balucani M, Fittipaldi R, Vecchione A, Attanasio C, 2009 EMRS Fall Meeting. Edited by EMRS. Warsaw: EMRS; 204, 2009.
[18].BandarenkaH, Redko S, Nenzi P, Balucani M, Nanotech, 2:269, 2011.
[19].P. Huber, Journal of nonmaterial's, Vol.2007, (2007).
[20].A.M. Alwan, O. A. Abdulrazaq, International Journal of Modern Physics B, Vol.22, 2008.

[21].G. Algun , M.C Arkian , Turkey Journal of Physics , Vol. 23 , 789-797, 1999.
[22]K.S. Khashan, Amany A. Awaad and Maysaa A. Mohamed, Engineering and Technology Journal, Vol.27, No.4, 663-674, 2008.
[23].N. Abass Ali Al-Temeeme,G.S. Muhammed, Advances in Materials Physics and Chemistry, Vol. 2, 55-58, 2012.